DOI: 10.1002/ejoc.200900511

Higher Aggregation of β-Peptide Networks Controlled by Nucleobase Pairing

Ratika Srivastava,[a] Anmol Kumar Ray,[a] and Ulf Diederichsen*[a]

Keywords: Aggregation / Peptides / Nucleobases / Helical structures / Structure elucidation / Self-assembly

The aggregation and 3D organization of peptide helices are key elements in biology but might also be relevant in nanostructure formation. β-Peptide helices were used as conformationally stable surrogates of α-peptides to be organized by covalently attached nucleobases as recognition units. Because the β-peptide 14-helix conformation allows addressing individual sides of the helix, the aggregation of helices functionalized on two helix flanks was investigated. Nine helices varying in sequence and nucleobase composition were prepared by solid-phase peptide synthesis and analyzed by temperature-dependent UV and CD spectroscopy and FT-ICR mass spectrometry. Already, sequences of three nucleobases on both sides of the helix provided stable aggregates. Aggregate formation was sequence dependent and led to one complex being stable in water at least up to 80 °C.

Introduction

Various synthetic oligomers with conformations similar to natural peptides and proteins have been studied extensively to increase the understanding of protein folding and stability.[1] Especially β-peptides have received considerable attention by many research groups as a result of their diversity in secondary structure formation. Six β-amino acids are sufficient to form stable secondary structures, whereas 15–20 α-amino acids are required for significant helix propensity.[2] In addition, β-peptides are stable in water and organic solvents as well as resistant towards enzymatic degradation.[3]

Helical secondary structures are most prominent in protein architecture.[4] They are widely involved in spatial organization, conformational reorganization, binding processes, and recognition between proteins or between proteins and nucleic acids.[5] β-Peptide secondary structures exist not only in organic solvents but also under physiological conditions.[6] Several helical secondary structures are known for β-peptides including the 14-helix, 12-helix, 10/12-helix, and 10-helix. Amongst them, the 14-helix is the most widely used helical secondary structure with three amino acids per turn and an orientation of every third amino acid residue (*i* and *i*+3) on the same side of the helix resulting in a linear arrangement of functionalities.[7] Conformationally constrained cyclic amino acids like *trans*-(1*R*,2*R*) 2-aminocyclohexanecarboxylic acid (ACHC) were used to achieve stable 14-helices,[8] and β-homolysine was incorporated to increase the solubility in aqueous media.[9]

Nucleobase-functionalized β-peptide 14-helices and their selective antiparallel organization by nucleobase recognition were reported previously.[10] Small β-peptide helices can be organized by nucleobase pairing gaining control over geometry, stoichiometry, and specificity of self association. Base pairing provides an excellent driving force for the self organization of 14-helices.[11] Incorporation of the nucleobases in positions *i* and *i*+3 leads to orientation of all nucleobases on one side of the helix. This preorganization of nucleobases on one face of the β-peptide helix facilitates helix–helix recognition by hydrogen bonding and stacking interactions.[12]

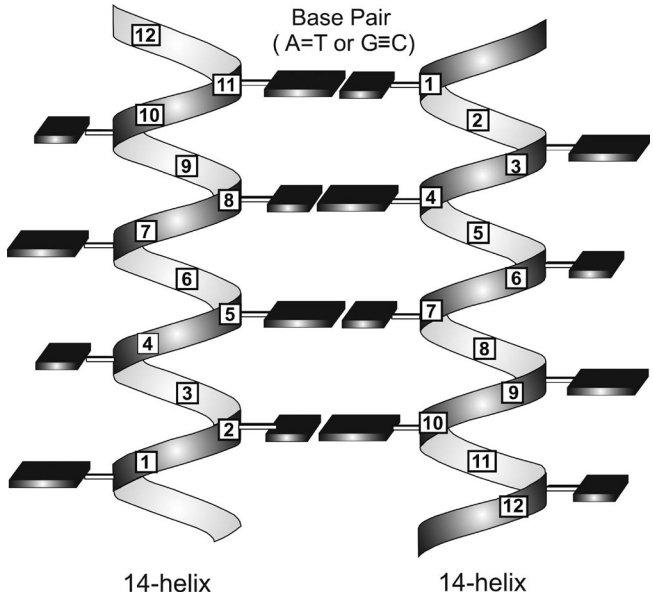

Figure 1. Antiparallel aggregation of β-peptide helices functionalized with nucleobases at two sides of the helix.

[a] Institut für Organische und Biomolekulare Chemie, Georg-August-Universität Göttingen,
Tammannstr. 2, 37077 Göttingen, Germany
Fax: +49-551-39-22944
E-mail: udieder@gwdg.de

Supporting information for this article is available on the WWW under http://dx.doi.org/10.1002/ejoc.200900511.

As an extension of this concept, it should be possible to organize β-peptide helices functionalizing two sides of a 14-helix by positioning nucleobases at *i*, *i*+3 and *i*+1, *i*+4, respectively (Figure 1). The current study is focused on β-peptides containing a proper choice of base sequences on both sides of the same helix in order to provide a well-defined molecular assembly.

Results and Discussion

Oligomers **1**–**9** containing nucleo-β-amino acids incorporated in every position *i* and *i*+3 for the first and every position *i*+1 and *i*+4 for the second nucleobase sequence were synthesized, respectively (Figure 2). The remaining positions of a turn were filled with the conformationally constrained cyclic residue ACHC and β-homolysine. These oligomers were composed of all four canonical nucleobases comparing the stabilities of base-pairing helices and the respective helical content. As known from the detection of other noncovalent biomolecules and hydrogen-bonding complexes, FT-ICR (ESI) mass spectrometry was successfully used to detect the aggregation of β-peptide 14-helices mediated by nucleobase functionalization on two sides of the helix.[13]

β-Peptide oligomers were synthesized by using solid-phase peptide synthesis at 50 °C on a 4-methylbenzhydrylamine polystyrene (MBHA) resin preloaded with homoglycine. The Boc-protected nucleo-β-amino acids were prepared by nucleophilic substitution at the side chain of β-homoserine derivatives or of a β-lactam methanesulfonate in case of the guaninyl nucleoamino acid.[14] Activation of the respective Boc-protected nucleo-β-amino acid was carried out by using [2-(7-aza-1*H*-benzotriazole-1-yl)-1,1,3,3-tetramethyluronium hexafluorophosphate] (HATU), 1-hydroxy-7-azabenzotriazole (HOAt), and Hünigs base in DMF. Oligomers were purified by HPLC, and the integrities of the β-peptide helices were confirmed by high-resolution FT-ICR mass spectrometry.

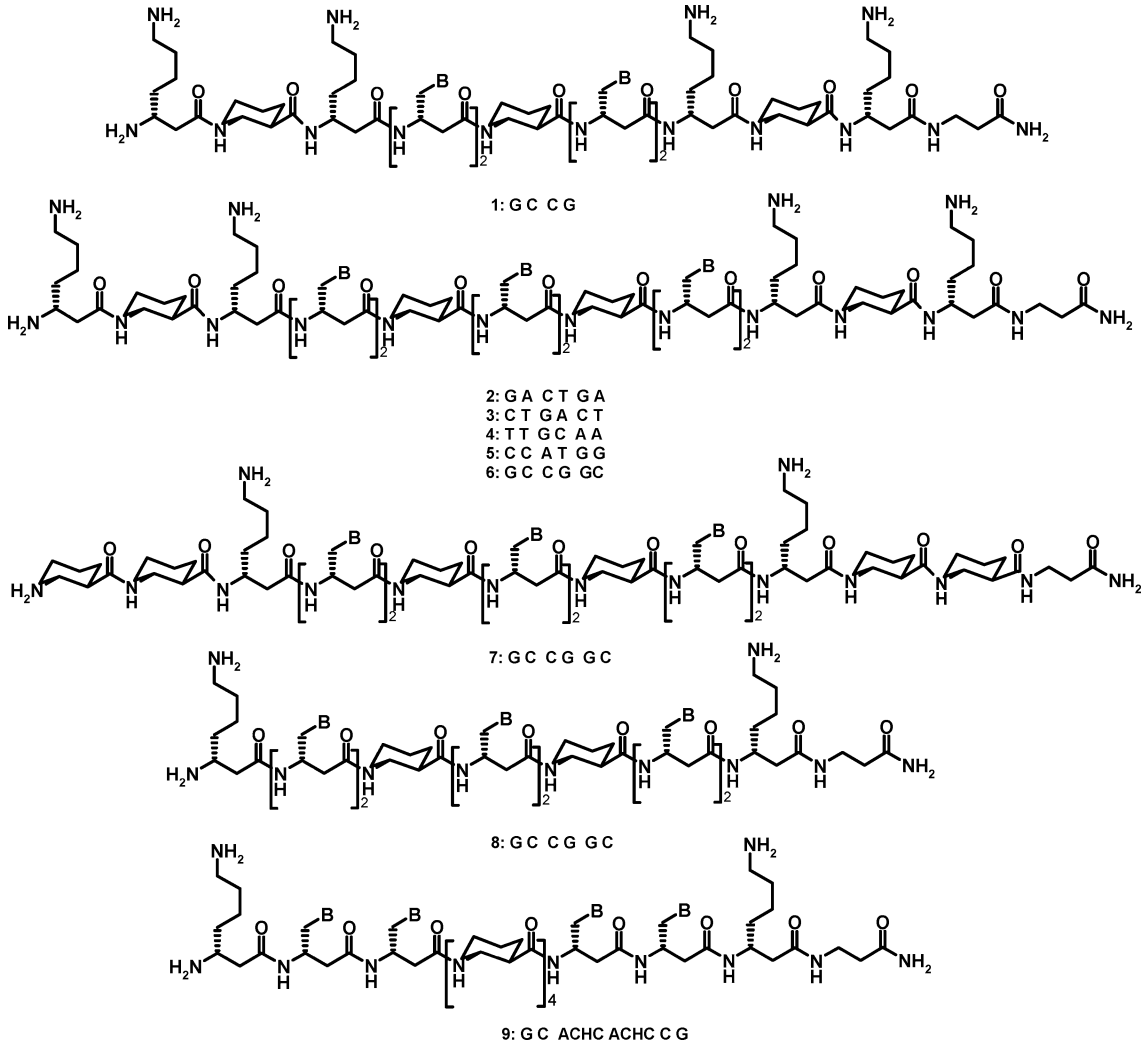

Figure 2. Nucleobase-modified β-peptide oligomers with nucleobase functionalization at two sides of the 14-helix.

β-Peptide Helix with Two G,C Recognition Units on Both Sides

First investigations of β-peptides functionalized with nucleobases on two sides were provided by synthesis of oligomer **1** containing guanine (G) and cytosine (C) recognition, each on two sides of the β-peptide helix. Watson–Crick pairing with three hydrogen bonds should be preferred for G–C recognition also in linear pairing topologies.[15] An intermolecular interaction between the G–C sequence from one helix side with the G–C sequence of the other side was expected with the preferred antiparallel helix orientation,[12] possibly leading to the formation of higher aggregates (Figure 3). First, it was proven that dodecamer **1** still provides the right-handed 14-helix, although four of the β-amino acids carry a nucleobase in the side chain. In accordance with previous studies the CD spectra of peptide **1** provided a strong positive Cotton effect at 215 nm that is indicative for the 14-helix (Figure 3). The helical content of oligomer **1** decreased at higher temperatures. The CD absorption between 250 to 300 nm correlates with the nucleobases conformationally oriented with respect to the helix, as it would be the case for interacting nucleobases. Interestingly, the maximum of the nucleobase-related Cotton effect was observed at 270 nm at higher temperatures as it is known for β-peptides that contain nucleobases only on one side of the helix;[12] at lower temperatures this maximum was shifted to 285 nm. The spectrum obtained by temperature-dependent measurement of the UV absorption of oligomer **1** at 260 nm indicated a sigmoidal transition that originates from recognizing oligomers with a stability of T_m = 20 °C [hyperchromicity (H) = 5%, 8 μM]. This transition was verified by the CD spectra obtained at different temperatures. At temperatures higher than 80 °C a second transition was indicated in accordance to the pronounced Cotton effect obtained for oligomer **1** at 80 °C. This high complex stability points to additional hydrogen-bond cross linking. Next to complementary canonical G–C pairing, the additional nucleobases on the other side of the helix or the guanine Hoogsteen side might be involved in additional aggregate formation.

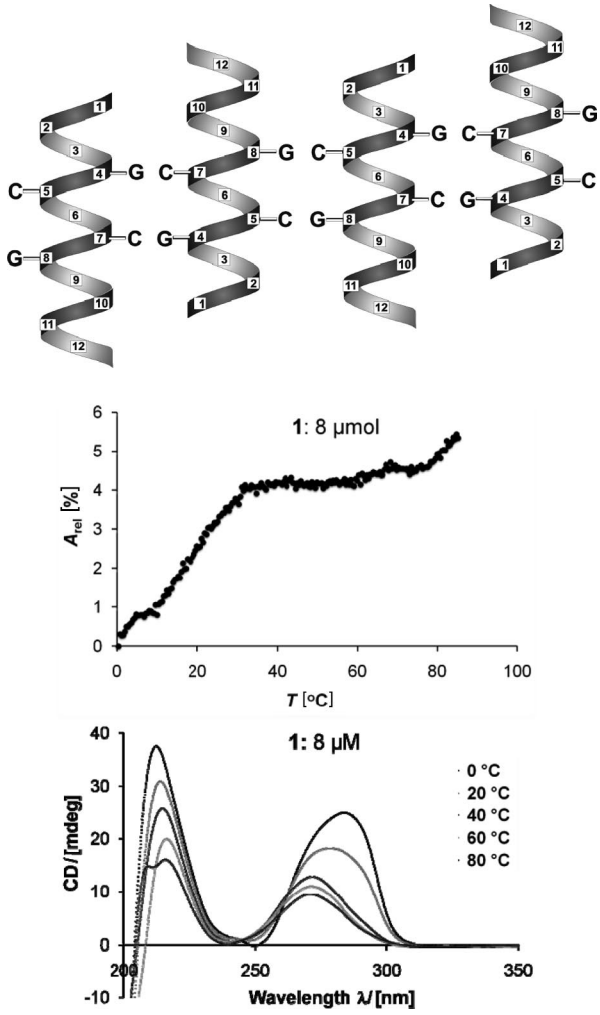

Figure 3. Schematic representation of antiparallel oriented β-peptide helices **1** being aggregated on the basis of base-pair recognition (top). Temperature-dependent UV (middle) and CD spectra (bottom) of oligomer **1** functionalized with G–C recognition on two sides of the 14-helix.

The doubly charged oligomer and quarterly charged dimer of oligomer **1** were detected by FT-ICR (ESI) mass spectrometry, whereas there was no evidence for higher aggregates (Supporting Information).

Helices with Different Non-Self-Complementary Recognition Sides

The second generation of two-sided nucleobase-modified 14-helices was elongated to provide higher helix propensity[16] and to obtain two sequences that are, on the one hand, not complementary to each other and, on the other hand, not self-complementary with all three nucleobases. Oligomers **2** (with the sequences GCG and ATA; A = adenine, T = thymine) and **3** (with the sequences CGC and TAT) fulfil these requirements; in addition, they are complementary to each other on both sides without restriction to antiparallel strand orientation (Figure 4). Providing a G–C and an A–T pairing side, the hydrogen-bonding recognition differs in the expected stability.

Because self-aggregation of oligomer **2** is possible with two base pairs, the determined stabilities of T_m = 27 °C (2%H, 8 μM) and T_m = 62 °C (2%H, 8 μM) are likely to reflect the self-association over the G–C and A–T side, respectively (Figure 5A). Alternatively, guanine tetrad formation over the purine-rich side might be possible.[17] The higher helix propensity contributes to the increase in stability compared to oligomer **1**.[12] In contrast, for oligomer **3** with lower purine content, only one melting transition was observed at T_m = 42 °C (10%H, 8 μM), which might reflect dimer formation based on two G–C base pairs or higher aggregate formation. In the CD spectra of oligomers **2** and **3**, stable 14-helices were indicated in both cases as well as evidence for the transitions that were shown by UV spectroscopy. In accordance with higher aggregate forma-

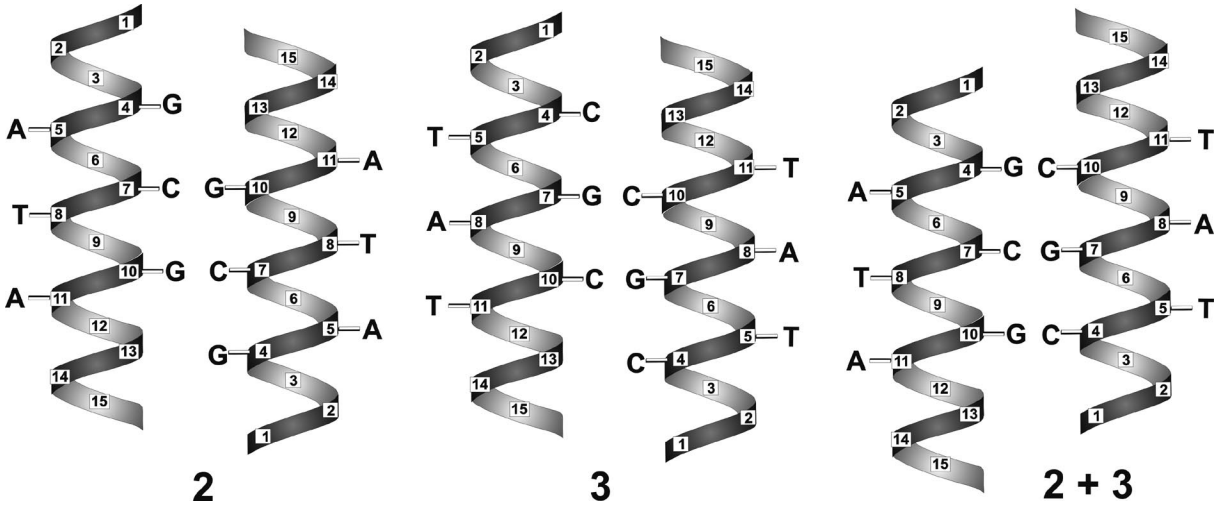

Figure 4. Schematic representation of self-pairing helices **2** and **3** and 1:1 complex of oligomers **2** and **3**.

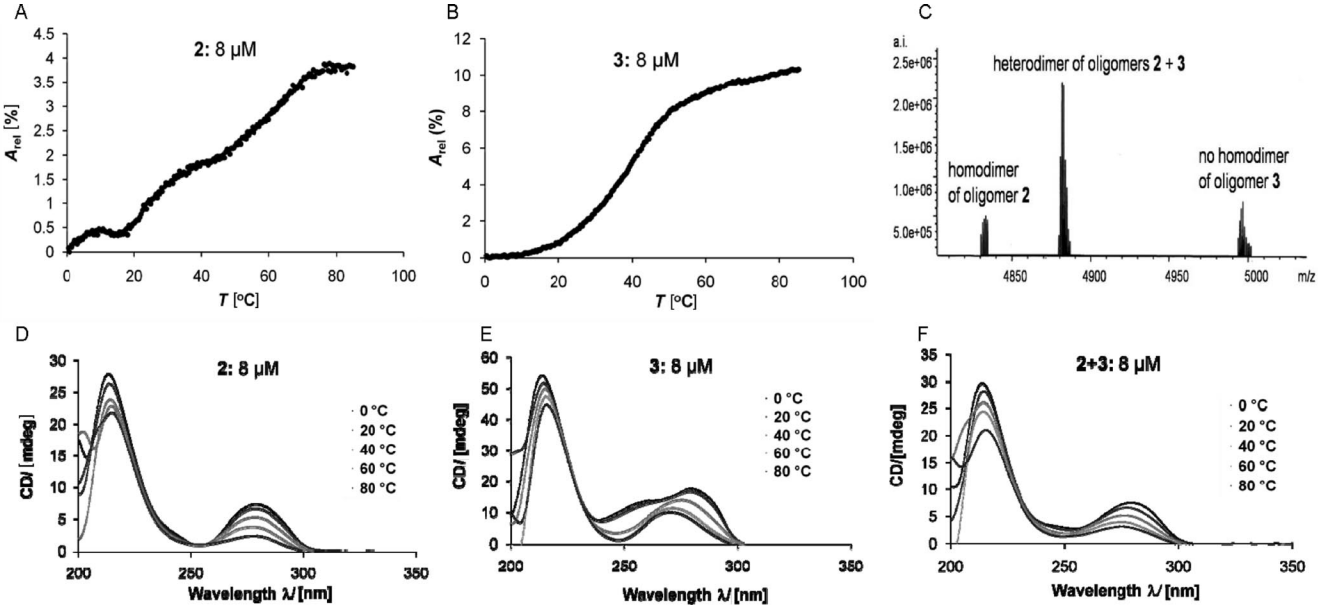

Figure 5. UV and CD spectra of homodimer complexes of oligomers **2** (A, D) and **3** (B, E). FT-ICR MS of an equimolar mixture of oligomers **2** and **3** (C) and CD spectrum of the heterocomplex (F).

tion, the low-temperature CD spectra of helix **3** also indicate significant broadening, shifting, and higher intensity of the Cotton effect between 240 and 300 nm.

The complementarity of oligomers **2** and **3** at the A–T and G–C sides was expected to lead to respective recognition complexes in an equimolar mixture of both oligomers (8 μM each, 5 mM NH_4OAc, pH 7.0). Indeed, the heterodimer was detected by FT-ICR MS (ESI) as the major component next to the homodimer of peptide **2** (Figure 5C). The formation of a heterodimer or higher aggregates between oligomers **2** and **3** was also indicated by temperature-dependent UV spectroscopy, providing a complex that is too stable to dissociate up to 80 °C (Supporting Information). The CD spectra of the equimolar mixture of oligomers **2** and **3** are in line with formation of a heterocomplex, showing a slight decrease in intensity combined with broadening of the bands, but apart from that a spectrum known from A–T, G–C pairing complexes (Figure 5D–F).

Helices with Two Self-Complementary Recognition Sides

Oligomers **4**–**6** differ from oligomers **2** and **3** only in the nucleobase sequence, as the sequences on both sides of the respective helix were designed to be complementary to each other assuming antiparallel strand orientation. The homodimer of oligomer **4** (with the sequences TGA and TCA) is based on two A–T and one G–C base pairs, the pairing complex of oligomer **5** (with the sequences CAG and CTG) on two G–C and one A–T base pairs (Figure 6), whereas

oligomer **6** (with the sequences GCG and CGC) can form three G–C base pairs. The stability of all self aggregating oligomers **4**–**6** was not detectable by temperature-dependent UV spectroscopy, as a slight nonsigmoidal decrease in the absorption was observed with increasing temperature (Supporting Information). If at all, G–C pairing oligomer **6** showed a small sigmoidal hypochromic effect (T_m = 62 °C, 2%H, 8 μM). The CD spectra of self-aggregating oligomers **4** and **5** indicate a very strong and shifted Cotton effect for the nucleobase region next to the well-established 14-helix (Figure 7A, B). This signal intensity is even more pronounced for oligomer **5** having the higher G–C content. In this respect, it is surprising that self-aggregation of β-peptide **6** also provides a strong Cotton effect in the base-pair region but not exceeding the effect of oligomer **5** and lacking the pronounced shift of the maximum towards higher wavelengths (Figure 7C). For G–C aggregating oligomers a more significant interaction was expected. Therefore, in a next step the variation of the peptide structure was investigated, keeping the G–C sequence of oligomer **6**.

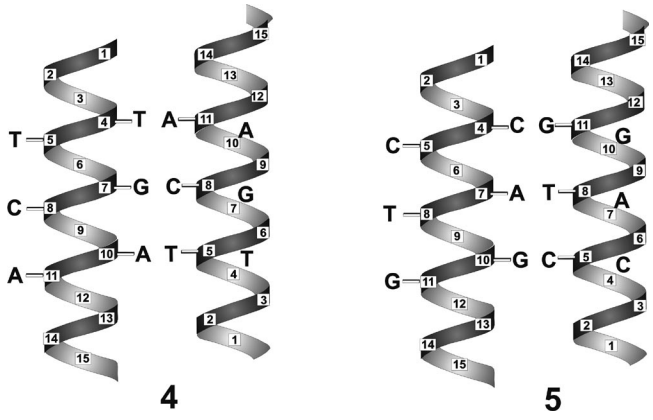

Figure 6. Schematic representation of self-pairing helices **4** and **5**.

Peptide Optimization for G–C Pairing 14-Helices

The influence of the amino acids at the termini of β-peptides might be of considerable influence on the 14-helical content and on the interaction between helices. Therefore, synthesis of β-peptide **7** was addressed to extend the 14-helical content by exchanging the two terminal homolysine amino acids of peptide **6** for ACHC units, thereby inducing higher helix propensity.[18] Unfortunately, the 14-helix conformation was partially disturbed also affecting the base pair interaction (Figure 8A). In contrast, oligomer **8** represents a truncated peptide missing the last two ACHC and homolysine amino acids of oligomer **6** otherwise keeping the sequence identical. For oligomer **8**, which is still soluble in aqueous buffer, it turned out that the helix propensity and the Cotton effect representing the base-pair region were enormously high; the Cotton effects remain nearly unchanged at least up to temperatures of 80 °C. This oligomer seems to be well stabilized by self-aggregation, as in FT-ICR MS, the intensity of remaining 14-helix **8** was about 100 times diminished compared to the other peptides. No dimer or other higher aggregates were detectable, leading to the conclusion that extensive aggregate formation provides particles that are too large to be transferred into the gas phase. In the UV melting profile of oligomer **8**, a hypochromic effect at T_m = 64 °C (7%H, 8 μM) is indicated as already known from oligomer **6** (Figure 9). Nevertheless, the higher aggregate formation with stabilities higher than

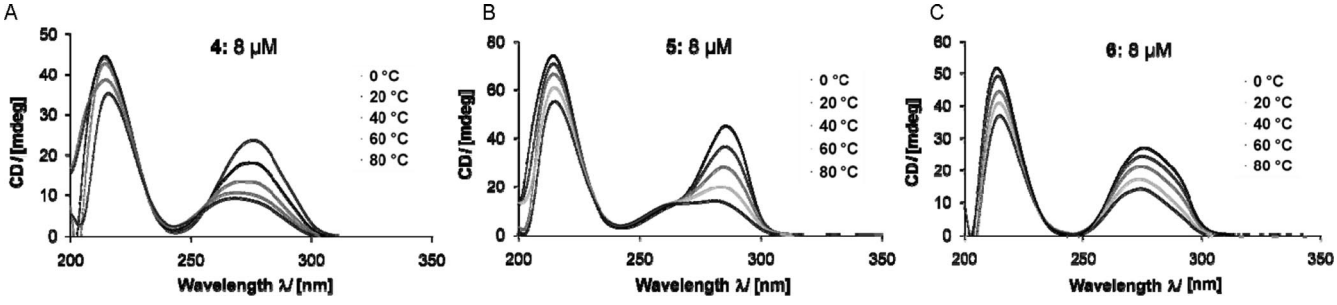

Figure 7. CD-spectra of self-aggregating complexes of oligomers **4**–**6**.

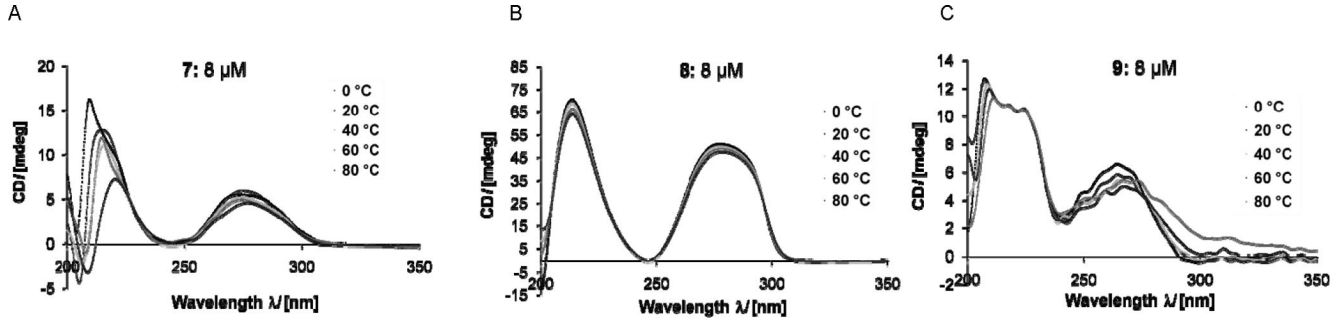

Figure 8. CD spectra of self-aggregating complexes of oligomers **7**–**9**.

80 °C is out of the detectable range of UV spectroscopy. Overall, there is distinct evidence from CD spectroscopy for a very stable higher aggregate being formed; indirectly, the data obtained by mass spectrometry and UV data are also in agreement with the higher aggregate, as a hyperchromic effect as expected for aggregating oligomers was missing in the measurable temperature range and the oligomers seem to be consumed in the aggregate not being available for transfer into the gas phase.

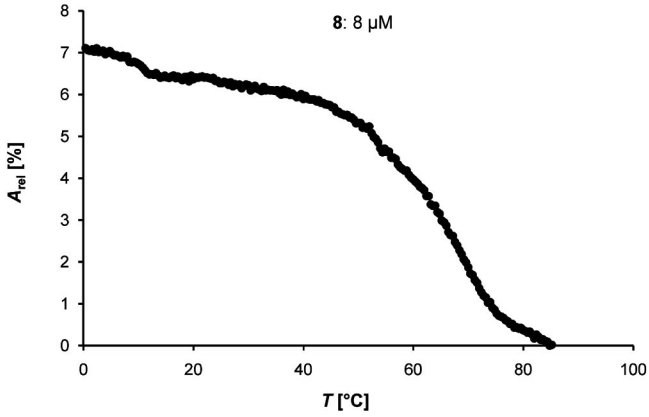

Figure 9. Temperature-dependent UV curve of G–C oligomer **8**.

Examining the possibilities of β-peptide helix **8** for aggregation based on antiparallel strand orientation and three G–C pairs each, there should be only one possible topology (Figure 10): A purine rich side needs to be recognized by a pyrimidine rich sequence resulting in a zigzag arrangement of helices. All helices are nicely aligned with respect to the dimension of the helix length, avoiding the drift that is indicated for self-aggregation of oligomer **1** or peptides **2** and **3**.

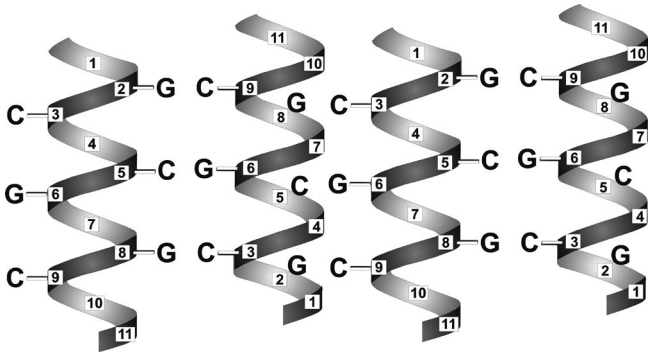

Figure 10. Schematic representation of self-pairing helices **8**.

Within the series of G–C pairing oligomers with peptide **9** an oligomer was investigated that lacks the central nucleobases. ACHC units were integrated in the middle of the oligomers instead of nucleo-β-amino acids leading to sequences G-ACHC-C and C-ACHC-G on the two flanks of the helix. With this oligomer the influence of noncontinuous stacking of nucleobases was investigated. Both recognition sides were complementary and the guanine side had the potential for further aggregation. Nevertheless, the discontinuities of nucleobases led to a nonsigmoidal decrease in the absorption. The CD spectra of peptide **9** provided a significantly diminished helical content and lower nucleobase organization (Figure 6C). Nevertheless, this oligomer preferred duplex formation, but also triplex formation was identified in FT-ICR MS (ESI), providing evidence for strong aggregation processes of nucleobase-substituted 14-helices.

The aggregation mode of β-peptide 14-helices with two recognition sides depends on base-pair recognition with the threefold G–C Watson–Crick hydrogen bonding being most favored. Furthermore, it was shown before that there is a clear preference for antiparallel orientation of interacting strands.[12] The antiparallel orientation is further enforced by the choice of interacting sequences. Therefore, the cyclic and band-like interacting modes (Figure 11) might be discussed as higher aggregates of nucleobase decorated β-peptide 14-helices. For G–C oligomer **8** it was concluded that band-like aggregation is facilitated by the nucleobase sequence. In contrast, oligomers like β-peptide **1** and oligomers **2** and **3** are candidates for cyclic arrangements (Figures 3 and 4). The suggested ring size involving six helices is based on the threefold geometry of a 14-helix and the antiparallel strand orientation requiring an even number of helices. The band-like aggregation mode is not restricted in aggregation size. In addition, it should be mentioned that further aggregate extension might be possible by overlapping sequences and aggregation in the helix axis direction.

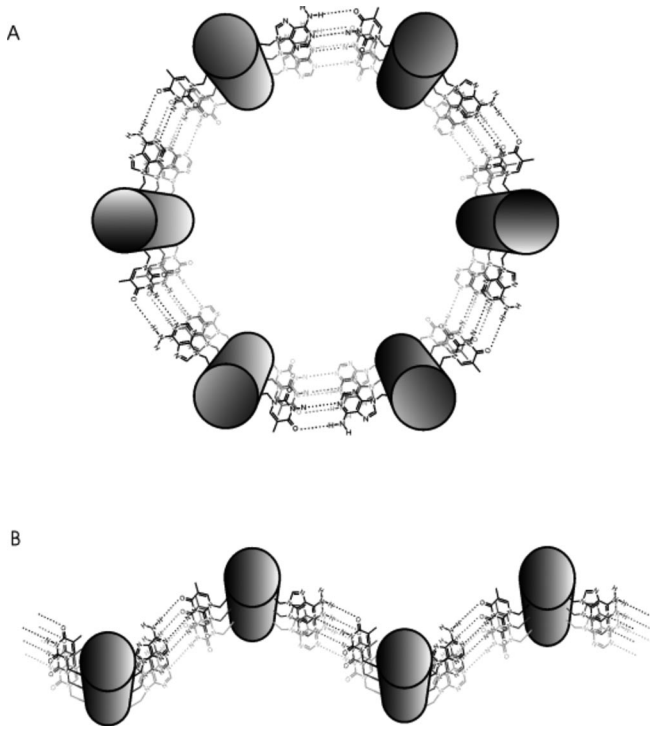

Figure 11. Possible modes of two-side nucleobase-functionalized β-peptide 14-helix aggregation.

Conclusions

β-Peptide 14-helices functionalized on two sides of the helix with nucleobase sequences show an excellent preorganization of the recognition units for specific recognition and simultaneous organization over both sides. As a result, higher aggregation of the helices can be obtained most likely organizing the helices in circles or band-like arrangements, even though the exact size of aggregates is still under investigation. Such an assembly of helices by nucleobase pairing could be of value in the construction of helical nanotubes, ion channels, and other macromolecular architectures.

Experimental Section

General: All reagents were of analytical grade and used without further purification. Highest-grade solvents were available. Dry solvents were stored over 4 Å molecular sieves. (1*R*,2*R*)-Boc-ACHC-OH was synthesized as mentioned in the literature.[19] Boc-β-HLys(*Z*)-OH was obtained by Arndt–Eistert homologation of the corresponding α-amino acid. Nucleo-β-amino acids Boc-β-HalA-OH, Boc-β-HalT-OH, Boc-β-HalG-OH, and Boc-β-HalC-OH were synthesized as described in the literature.[10,14] The 4-methylbenzhydrylamine polystyrene (MBHA-PS) resin was purchased from Novabiochem. Purification and HPLC analysis of the oligomers was performed with a Pharmacia Äkta basic (pump type P-900, variable wavelength detector type UV-900) with a linear gradient of A (0.1% TFA in H_2O) to B (MeCN/H_2O, 9:1 + 0.1 TFA). Oligomers were purified on a J'sphere column ODS-H80, RP-C18; 150 × 4.6 mm, 4 μm, 80 Å with a flow rate of 1 mL min^{-1} or YMC J'sphere column ODS-H80, RP-C18; 250 × 4.6 mm, 4 μm, 80 Å at a flow rate of 1 mL min^{-1} for analytical samples and preparative samples were purified on J'sphere column ODS-H80, RP-C18; 150 × 10 mm, 4 μm, 80 Å with a flow rate of 3 mL min^{-1} or YMC J'sphere column ODS-H80, RP-C18; 250 × 20 mm, 4 μm, 80 Å with a flow rate of 10 mL min^{-1}. Mass spectra were recorded with a LCG Finnigan spectrometer. High-resolution mass spectra were recorded with a Bruker APEX-IV FT ICR mass spectrometer. A JASCO J-810 spectropolarimeter equipped with a JASCO ETC-505S/ETC-505T temperature controller was used to record the CD spectra. All the measurements were carried out in 10 mM Tris·HCl buffer (pH = 7.5) in a quartz cell of 1 cm path length. Spectra represent the average of four scans after baseline correction. Temperature-dependent UV spectra were measured with a JASCO V-550 UV/Vis spectrometer equipped with JASCO ETC-505S/ETC-505T temperature controller. All measurements were carried out in a quartz cell of 1 cm path length in 10 mM Tris·HCl buffer (pH = 7.5). Data were collected at 260 nm at a heating rate of 0.5 °C min^{-1} in a quartz cell of 1 cm path length. Prior to recording the spectroscopic data annealing of the oligomer samples was performed by heating to 80 °C, cooling to 0 °C within 30 min, and keeping the sample at this temperature for 15 min. Oligomer concentrations were determined on the basis of the absorption at 260 nm. The extinction coefficient of each oligomer was the sum of the extinction coefficients of the contained nucleobases.[20]

General Procedure for Solid-Phase β-Peptide Synthesis: β-Peptides were synthesized manually by solid-phase peptide synthesis in a small fritted glass column (Ø = 1.5 cm). 4-Methylbenzhydrylamine polystyrene resin (loading capacity: 0.59 mmol g^{-1}) was preloaded with Boc-β-HGly-OH (30 mg, 17.7 μmol). Solid-phase synthesis of oligomers was performed by coupling of the amino acids at 50 °C. An excess amount of β-amino acid (88.5 μmol, 5 equiv.) was preactivated with HATU (79.7 μmol, 4.5 equiv.), HOAt (0.5 M in DMF, 88.5 μmol, 5 equiv.), and *N*,*N*-diisopropylethylamine (248 μmol, 14 equiv.) in dry DMF (400 μL). The second coupling was performed with β-amino acid (53.1 μmol, 3 equiv.) and activation with HATU (47.8 μmol, 2.7 equiv.), HOAt/DMF (35.4 μmol, 2 equiv.), and DIEA (106 μmol, 6 equiv.) in DMF (400 μL). After swelling of the loaded resin for 2 h in CH_2Cl_2 (2 mL), the following steps were repeated for each coupling: (i) deprotection twice for 3 min with TFA/*m*-cresol (95:5, 2 mL); (ii) washing five times with CH_2Cl_2/DMF (1:1, 2 mL) and then five times with pyridine (2 mL); (iii) double coupling steps, each 1 h gentle moving at 50 °C; (iv) washing with CH_2Cl_2/DMF (1:1, 3 × 2 mL), DMF/piperidine (95:5, 3 × 2 mL), and CH_2Cl_2/DMF (1:1, 2 mL), (v) two times capping for 3 min with DMF/Ac_2O/DIEA (8:1:1, 2 mL). After the last coupling step, the resin was washed with TFA (3 × 2 mL) and CH_2Cl_2 (5 × 2 mL) and dried in vacuo overnight. The resin was transferred into a small flask and was suspended with *m*-cresol/thioanisole/ethanedithiol (2:2:1, 500 μL). After stirring at room temperature for 30 min, TFA (2 mL) was added, and the reaction mixture was cooled to –20 °C. Trifluoromethanesulfonic acid (TFMSA) (200 μL) was added dropwise with vigorous stirring. The mixture was warmed to room temperature in 1.5 h and was stirred for another 2 h. The mixture was filtered through a fritted glass funnel and TFA was removed under reduced pressure. The crude oligomer was obtained by precipitation from cold ethyl ether (–15 °C) and dried in vacuo. The crude peptide was dissolved in a water/CH_3CN mixture, filtered, and purified by preparative HPLC.

H-(β-HLys-ACHC-β-HLys-β-HalG-β-HalC-ACHC-β-HalC-β-HalG-β-HLys-ACHC-β-HLys-HGly)-NH$_2$ (1): HPLC (RP-C18, 150 × 4.6 mm); t_R = 15.3 min, gradient: 5% to 50% in 30 min. MS (ESI): *m*/*z* = 630.37 [M + 3H]$^{3+}$, 945.56 [M + 2H]$^{2+}$, 1890.10 [M + H]$^{+}$. HRMS: calcd. for $C_{86}H_{137}N_{33}O_{16}$ [M + 3H]$^{3+}$ 630.37131; found 630.37151.

H-(β-HLys-ACHC-β-HLys-β-HalG-β-HalA-ACHC-β-HalC-β-HalT-ACHC-β-HalG-β-HalA-β-HLys-ACHC-β-HLys-HGly)-NH$_2$ (2): HPLC (RP-C18, 150 × 4.6 mm); t_R = 16.81 min, gradient: 5% to 60% in 30 min. MS (ESI): *m*/*z* = 617.09 [M + 4H]$^{4+}$, 822.46 [M + 3H]$^{3+}$, 2466.38 [M + H]$^{+}$. HRMS: calcd. for $C_{112}H_{169}N_{45}O_{20}$ [M + 3H] $^{3+}$ 822.46029; found 822.46003.

H-(β-H-Lys-ACHC-β-HLys-β-HalC-β-HalT-ACHC-β-HalG-β-HalA-ACHC-β-HalC-β-HalT-β-HLys-ACHC-β-HLys-HGly)-NH$_2$ (3): HPLC (RP-C18, 150 × 4.6 mm); t_R = 15.74 min, gradient: 5% to 60% in 30 min. MS (ESI): *m*/*z* = 605.10 [M + 4H]$^{4+}$, 806.46 [M + 3H]$^{3+}$, 1209.18 [M + 2H]$^{2+}$, 2417.36 [M + H]$^{+}$. HRMS: calcd. for $C_{111}H170N_{40}O_{22}$ [M + 4H]$^{4+}$ 605.0934; found 605.09344.

H-(β-H-Lys-ACHC-β-HLys-β-HalT-β-HalT-ACHC-β-HalG-β-HalC-ACHC-β-HalA-β-HalA-β-HLys-ACHC-β-HLys-HGly)-NH$_2$ (4): HPLC (RP-C18, 150 × 4.6 mm); t_R = 17.5 min, gradient: 5% to 60% in 30 min. MS (ESI): *m*/*z* = 611.10 [M + 4H]$^{4+}$, 814.46 [M + 3H]$^{3+}$, 2441.36 [M + H]$^{+}$. HRMS: calcd. for $C_{112}H_{170}N_{42}O_{21}$ [M + 4H]$^{4+}$ 610.84542; found 610.84584.

H-(β-H-Lys-ACHC-β-HLys-β-HalC-β-HalC-ACHC-β-HalA-β-HalT-ACHC-β-HalG-β-HalG-β-HLys-ACHC-β-HLys-HGly)-NH$_2$ (5): HPLC (RP-C18, 150 × 4.6 mm); t_R = 16.37 min, gradient: 5% to 60% in 30 min. MS (ESI): *m*/*z* = 611.34 [M + 4H]$^{4+}$, 814.79 [M + 3H]$^{3+}$, 2442.34 [M + H]$^{+}$. HRMS: calcd. for $C_{111}H_{169}N_{43}O_{21}$ [M + 4H]$^{4+}$ 611.34567; found 611.34521.

H-(β-H-Lys-ACHC-β-HLys-β-HalG-β-HalC-ACHC-β-HalC-β-HalG-ACHC-β-HalG-β-HalC-β-HLys-ACHC-β-HLys-HGly)-NH$_2$ (6): HPLC (RP-C18, 150 × 4.6 mm); t_R = 14.87 min, gradient: 5%

to 60% in 30 min. MS (ESI): *m/z* = 611.60 $[M + 4H]^{4+}$, 815.12 $[M + 3H]^{3+}$, 1221.68 $[M + 2H]^{2+}$, 2443.36 $[M + H]^{+}$. HRMS: calcd. for $C_{110}H_{168}N_{44}O_{21}$ $[M + 2H]^{2+}$ 1221.67881; found 1221.67870.

H-(ACHC-ACHC-β-HLys-β-HalG-β-HalC-ACHC-β-HalC-β-HalG-ACHC-β-HalG-β-HalC-β-HLys-ACHC-ACHC-HGly)-NH_2 (7): HPLC (RP-C18, 250×4.6 mm); t_R = 18.22 min, gradient: 5% to 60% in 30 min. MS (ESI): *m/z* = 803.43 $[M + 3H]^{3+}$, 1204.65 $[M + 2H]^{2+}$, 2407.30 $[M + H]^{+}$. HRMS: calcd. for $C_{110}H_{162}N_{42}O_{21}$ $[M + 3H]^{3+}$ 803.43727; found 803.43717.

H-(β-HLys-β-HalG-β-HalC-ACHC-β-HalC-β-HalG-ACHC-β-HalG-β-HalC-β-HLys-HGly)-NH_2 (8): HPLC (RP-C18, 250×4.6 mm); t_R = 16.48 min, gradient: 5% to 60% in 30 min. MS (ESI): *m/z* = 636.65 $[M + 3H]^{3+}$, 945.58 $[M + 2H]^{2+}$, 1907.96 $[M + H]^{+}$. HRMS: calcd. for $C_{82}H_{118}N_{38}O_{17}$ $[M + 4H]^{4+}$ 477.74571; found 477.74569.

H-(β-HLys-β-HalG-β-HalC-ACHC-ACHC-ACHC-ACHC-β-HalC-β-HalG-β-HLys-HGly)-NH_2 (9): HPLC (RP-C18, 250×4.6 mm); t_R = 16.48 min, gradient: 5% to 60% in 30 min. MS (ESI): *m/z* = 433.24 $[M + 4H]^{4+}$, 577.32 $[M + 3H]^{3+}$. HRMS: calcd. for $C_{79}H_{120}N_{30}O_{15}$ $[M + 4H]^{4+}$ 433.24601; found 433.24602.

Supporting Information (see footnote on the first page of this article): FT-ICR MS evidence for aggregate formation of helices **1**–**9** and temperature-dependent UV spectra of oligomers **2**–**6**.

Acknowledgments

Generous support of the Deutsche Forschungsgemeinschaft (GRK 782) is gratefully acknowledged.

[1] a) M. S. Cubberly, B. L. Iverson, *Curr. Opin. Struct. Biol.* **2001**, *5*, 650–653; b) K. P. Howard, J. D. Lear, W. F. DeGrado, *Proc. Natl. Acad. Sci. USA* **2002**, *99*, 8568–8572; c) X. Li, Y. D. Wu, D. Yang, *Acc. Chem. Res.* **2008**, *41*, 1428–1438.
[2] U. Koert, *Angew. Chem. Int. Ed. Engl.* **1997**, *36*, 1836–1837.
[3] J. Franckénpohl, P. I. Arvidson, J. V. Schreiber, D. Seebach, *ChemBioChem* **2001**, *2*, 445–455.
[4] a) M. Suzuki, J. Suckow, B. Kisters-Woike, H. Aramaki, K. Makino, *Adv. Biophys.* **1996**, *32*, 31–52; b) R. T. Sauer, *Nat. Struct. Biol.* **1995**, *2*, 7–9; c) R. L. Stanfield, I. A. Wilson, *Curr. Opin. Struct. Biol.* **1995**, *5*, 103–113.
[5] a) K. Nakagawa, Y. Yamada, K. Fujiwara, M. Ikeguchi, *J. Mol. Biol.* **2007**, *367*, 1205–1214; b) A. J. Nicoll, D. J. Miller, K. Fütterer, R. Ravelli, R. K. Allemann, *J. Am. Chem. Soc.* **2006**, *128*, 9187–9193; c) A. P. Demchenko, *J. Mol. Recognit.* **2001**, *14*, 42–61.
[6] W. F. DeGrado, J. P. Schneider, Y. Hamuro, *J. Pept. Res.* **1999**, *54*, 206–217.
[7] a) D. H. Appella, J. J. Barchi, S. R. Durell, S. H. Gellman, *J. Am. Chem. Soc.* **1999**, *121*, 2309–2310; b) P. I. Arvidsson, M. Rueping, D. Seebach, *Chem. Commun.* **2001**, 649–650.
[8] a) T. L. Raguse, J. R. Lai, S. H. Gellman, *Helv. Chim. Acta* **2002**, *85*, 4145–4164; b) T. L. Raguse, E. A. Porter, B. Weisblum, S. H. Gellman, *J. Am. Chem. Soc.* **2002**, *124*, 12774–12785; c) T. L. Raguse, J. R. Lai, S. H. Gellman, *J. Am. Chem. Soc.* **2003**, *125*, 5592–5593.
[9] J. V. N. Vara Prasad, J. A. Loo, F. E. Boyer, M. A. Stier, R. D. Gogliotti, W. J. Turner, P. J. Harvey, M. R. Kramer, D. P. Mack, J. D. Scholten, S. J. Gracheck, J. M. Domagala, *Bioorg. Med. Chem.* **1998**, *6*, 1707–1730.
[10] a) A. Weiß, U. Diederichsen, *Eur. J. Org. Chem.* **2007**, 5531–5539; b) P. Chakraborty, A. M. Brückner, U. Diederichsen, *Eur. J. Org. Chem.* **2006**, 2410–2416.
[11] A. M. Brückner, P. Chakraborty, S. H. Gellman, U. Diederichsen, *Angew. Chem. Int. Ed.* **2003**, *42*, 4395–4399.
[12] P. Chakraborty, U. Diederichsen, *Chem. Eur. J.* **2005**, *11*, 3207–3216.
[13] a) A. G. Marshall, C. L. Hendrickson, G. S. Jackson, *Mass Spectrom. Rev.* **1998**, *17*, 1–35; b) S. A. Poulsen, P. G. Gates, G. R. L. Cousins, J. K. M. Sanders, *Rapid Commun. Mass Spectrom.* **2000**, *14*, 44–48; c) A. G. Marshall, C. L. Hendrickson, *Int. J. Mass Spectrom.* **2002**, *215*, 59–75; d) R. Iwaura, M. Ohnishi-Kameyamab, M. Yoshidab, T. Shimizu, *Chem. Commun.* **2002**, 2658–2659; e) B. Abel, A. Charvat, U. Diederichsen, M. Faubel, A. Zeeck, *Int. J. Mass Spectrom.* **2005**, *243*, 177–188.
[14] A. M. Brückner, H. W. Schmitt, U. Diederichsen, *Helv. Chim. Acta* **2002**, *85*, 3855–3866.
[15] a) U. Diederichsen, *Angew. Chem. Int. Ed. Engl.* **1997**, *36*, 1886–1889; b) U. Diederichsen, D. Weicherding, N. Diezemann, *Org. Biomol. Chem.* **2005**, *3*, 147–153.
[16] a) N. Rathore, S. H. Gellman, J. J. de Pablo, *Biophys. J.* **2006**, *91*, 3425–3435; b) M. R. Lee, T. L. Raguse, M. Schinnerl, W. C. Pomerantz, X. Wang, P. Wipf, S. H. Gellman, *Org. Lett.* **2007**, *9*, 1801–1804.
[17] a) J.-L. Mergny, A.-T. Phan, L. L. Lacroix, *FEBS Lett.* **1998**, *435*, 74–78; b) Y. Krishnan-Ghosh, D. Liu, S. Balasubramanian, *J. Am. Chem. Soc.* **2004**, *126*, 11009–11016.
[18] a) D. H. Appella, L. A. Christianson, I. L. Karle, D. R. Powell, S. H. Gellman, *J. Am. Chem. Soc.* **1996**, *118*, 13071–13072; b) J. J. Barchi, X. L. Huang, D. H. Appella, L. A. Christianson, A. R. Durell, S. H. Gellman, *J. Am. Chem. Soc.* **2000**, *122*, 2711–2718.
[19] M. Schinnerl, J. K. Murrary, J. M. Langenhan, S. H. Gellman, *Eur. J. Org. Chem.* **2003**, 721–726.
[20] a) H. J. Galla, *Spektroskopische Methoden in der Biochemie*, Thieme, Stuttgart, **1988**; b) M. G. Gore, *Spectrophotometry and Spectrofluorometry: A Practical Approach*, University Press Inc., New York, **2000**.

Received: May 7, 2009
Published Online: August 26, 2009

